Pergamon

PII: S0021-9290(96)00062-0

J. Biomechanics, Vol. 29, No. 10, pp. 1309–1317, 1996

Printed in Great Britain
0021-9290/96 $15.00 + .00

THE DEPENDENCE OF SHEAR FAILURE PROPERTIES OF TRABECULAR BONE ON APPARENT DENSITY AND TRABECULAR ORIENTATION

Catherine M. Ford* and Tony M. Keaveny†, ‡

* Orthopaedic Biomechanics Laboratory, Department of Orthopaedic Surgery, Charles A. Dana Research Institute, Harvard Thorndike Laboratory, Beth Israel Hospital and Harvard Medical School, 330 Brookline Avenue, Boston, Massachusetts, U.S.A.; †Orthopaedic Biomechanics Laboratory, Department of Mechanical Engineering, University of California, Berkeley, California, U.S.A.; and ‡Department of Orthopaedic Surgery, University of California, San Francisco, California, U.S.A.

Abstract—The shear properties of trabecular bone, in particular the shear failure strains, are not well understood despite their potential importance in age-related fractures and prosthesis loosening. We hypothesized that shear failure strains (yield and ultimate) are independent of apparent density and trabecular orientation, i.e. are homogeneous and isotropic. We measured the shear failure properties of bovine tibial trabecular bone, where specimens were loaded to failure in torsion longitudinally ($n = 25$) or transversely ($n = 23$) relative to the primary trabecular orientation. We found that although failure stresses depended strongly on apparent density ($r^2 = 0.61 - 0.80$), failure strains were independent of apparent density for both trabecular orientations. Although the mean ($\pm$ S.D.) yield strain in the longitudinal group ($1.46 \pm 0.19\%$) was 10% higher ($p = 0.01$) than in the transverse group ($1.33 \pm 0.15\%$), indicating a slight anisotropy of shear yield strains, the mean ultimate strains did not depend on trabecular orientation (longitudinal group $4.60 \pm 0.77\%$ vs transverse group $4.24 \pm 1.25\%$, $p = 0.20$). These findings indicate that shear failure strains are homogeneous and largely isotropic. By combining our shear data with compressive data from a previous experiment, we also predicted that trabecular bone can fail in shear when subjected to compressive loads that are not aligned with the principal trabecular orientation. If this prediction holds for human bone, shear may be a dominant failure mode during off-axis loading of trabecular bone *in vivo*, such as during falls on the hip. Copyright © 1996 Elsevier Science Ltd.

Keywords: Bone; Trabecular; Shear; Strain; Strength.

INTRODUCTION

Prediction of trabecular bone failure during *in vivo* loading, which is essential for prosthesis design and fracture risk assessment, requires accurate knowledge of its shear failure properties. If the high shear stresses which exist near prostheses (Cheal *et al.*, 1992) exceed the shear strength of trabecular bone, prosthesis loosening may occur. Since falls can induce multiaxial stresses in the proximal femur (Lotz *et al.*, 1991), hip fracture risk prediction also requires knowledge of shear failure properties, which directly affect multiaxial strength (Tsai and Wu, 1971). Since trabecular bone in load-bearing skeletal regions is adapted to transmit compressive and tensile loads along its primary orientation during habitual activities, shear failure may play a large role in trabecular bone fracture during traumatic loads which are not aligned with the primary orientation.

There is mounting evidence that failure strains for tensile (Rohl *et al.*, 1991; Keaveny *et al.*, 1994c) and compressive (Hvid *et al.*, 1985; Hansson *et al.*, 1987; Mosekilde *et al.*, 1987; Hvid *et al.*, 1989; Keaveny *et al.*, 1994c) loading of trabecular bone are homogeneous (independent of apparent density and modulus) and isotropic (independent of trabecular orientation, Turner, 1989; Keaveny *et al.*, 1994b), suggesting that trabecular bone failure is fundamentally a function of the strain that the bone experiences, rather than the stress. However, previous investigations of the *shear* failure properties of trabecular bone have focused exclusively on *stresses* at failure (Halawa *et al.*, 1978; Saha and Gorman, 1981; Stone *et al.*, 1983), such that there is currently a lack of knowledge about shear failure *strains*. In addition, there is a lack of information regarding relationships between shear failure properties (both stresses and strains) and trabecular orientation. Knowledge of these relationships would provide considerable insight into whether trabecular bone failure *in vivo* is due primarily to shear or to normal strains, both for when the bone is subjected to habitual loading or to traumatic, off-axis loading. If trabecular bone failure during off-axis loading occurs primarily in shear, this result many have substantial implications for predicting age-related fracture risk and evaluating the structural consequences of osteoporosis.

We hypothesized that shear failure strains (yield and ultimate) in trabecular bone are homogeneous, and that by contrast to shear failure stresses which are anisotropic, shear failure strains are isotropic. We also hypothesized that shear is a dominant failure mode when trabecular bone is loaded obliquely relative to its

Received in final form 15 *February* 1996.
Address correspondence to: Tony M. Keaveny, Dept. of Mechanical Engineering, 6175 Etcheverry Hall University of California, Berkeley, CA 94720-1740, U.S.A.

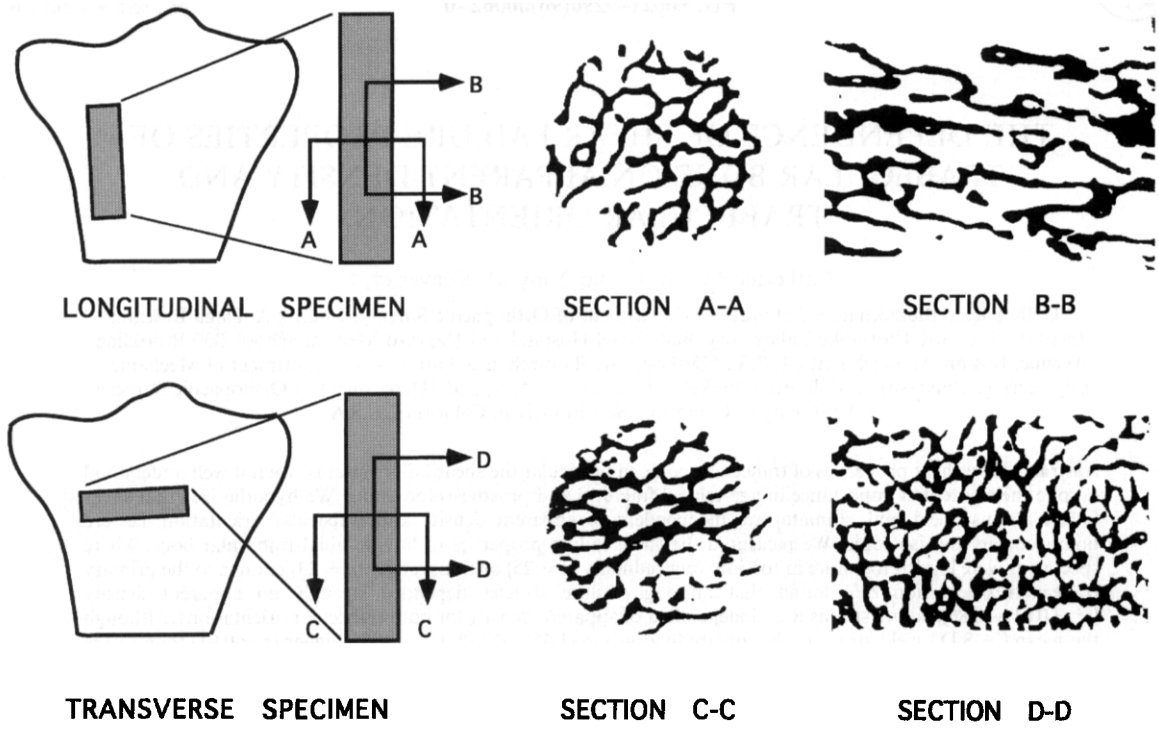

Fig. 1. Sections of typical trabecular bone specimens (bone is black) from longitudinal (top) and transverse (bottom) groups. Longitudinal specimens, where the primary trabecular orientation was parallel to the long axis of the specimen (Section B–B), were typically harvested from the anterior and posterior aspects of the tibia and the long axis of the specimen was approximately aligned with the long axis of the tibia. Transverse specimens, where the primary trabecular orientation was perpendicular to the long axis of the specimen (Section D–D), were typically harvested from the central aspect of the tibia, with the long axis of the specimen perpendicular to the long axis of the tibia. The similarity in architecture between Sections A–A and D–D, which appear isotropic, combined with the similarity between Sections B–B and C–C, which appear aligned, demonstrates that the architecture of the bone in both groups was approximately transversely isotropic.

primary trabecular orientation. To test our hypotheses, we sought to: (1) determine the dependence of shear failure stresses and failure strains on apparent density and shear modulus by testing cylindrical specimens of bovine tibial trabecular bone to failure in torsion; (2) compare magnitudes of shear failure stresses and strains for specimens with longitudinal vs transverse trabecular orientations; and (3) use our shear data, combined with compressive and tensile data (Keaveny *et al.*, 1994c), to investigate the dominant failure modes when compressive loads are applied obliquely relative to the primary trabecular orientation.

MATERIALS AND METHODS

Thirty-nine tibiae from 1–2-yr-old cows were obtained from a slaughterhouse (Bertolino Beef Company, Boston, MA). Reduced-section cylindrical specimens, used to bias failure toward a region of uniform surface stress, were prepared according to our published protocol (Keaveny *et al.*, 1994a). Briefly, saggital and coronal plane sections of bovine proximal tibiae were radiographed to identify regions of longitudinally and transversely oriented trabecular bone (Fig. 1). Parallelepipeds were cut from well-oriented regions, and 40 mm long, 8.3 diameter cylinders were obtained using a diamond-tipped coring tool (#102095, Starlite, Rosemont, PA) at 360 rpm . The specimen ends were cleaned, dried, and press-fit with cyanoacrylate (Prism 401, Loctite, Newington, CT) into aligned brass end-caps. After freezing for 3 h at −70°C, the central 18 mm section was turned down at 315 rpm to a diameter of 6 mm. Microscopic analysis has demonstrated that no obvious damage occurs to surface trabeculae during this machining process (Keaveny *et al.*, 1994a). All but the embedded ends of the specimens were kept wet during preparation and testing. Twenty-eight longitudinal and 26 transverse specimens were produced in this manner. Of the 39 tibiae used, 17 of the bones yielded only longitudinal specimens, 20 of the bones yielded only transverse specimens, and 2 bones yielded both longitudinal and transverse specimens. Due to the arrangement of trabecular bone within the bovine proximal tibia, longitudinal specimens tended to come from the anterior and posterior aspects, and transverse specimens generally came from closer to the central aspect. Despite the potential bias introduced by this slight difference in harvest locations, serial sectioning of a random

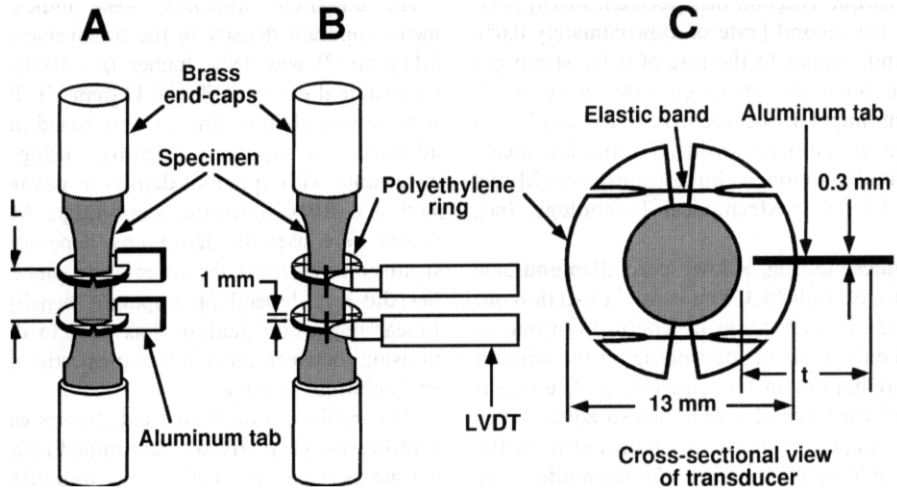

Fig. 2. Schematic of rotational transducer system used to measure shear strain on specimen surface (not to scale). Each 40 mm long, 8.3 mm diameter trabecular bone core was glued into brass endcaps approximately 25 mm apart, and the central 18 mm length was turned down to a diameter of 6 mm. Two 1 mm thick, split polyethylene rings were mounted to the gage length of each specimen ($L \approx 6$ mm nominally) using orthodontic elastic bands. A 0.3 mm thick aluminum tab perpendicular to each ring was used to couple the angular displacement of the specimen surface to the deflection of a linearly variable differential transformer (LVDT), positioned perpendicularly at a distance $t = 8$ mm from the edge of the specimen. (A) View of rotational transducer system showing setup without LVDT's. (B) Perpendicular view, showing LVDT placement. (C) Top view detail of split polyethylene ring, showing attachment to specimen via orthodontic elastic bands.

subset of specimens revealed that trabecular architectures within the two groups were similar, and each were approximately transversely isotropic (Fig. 1).

To measure shear strain on the reduced section of each specimen, a rotational displacement transducer system was designed (Fig. 2). This system included two 1 mm thick, 13 mm diameter split polyethylene rings, attached 6 mm apart to the specimen gage length using orthodontic elastic bands. A 0.3 mm thick aluminum tab perpendicular to each ring was used to couple the rotation at the specimen surface to the deflection of a linear variable differential transformer (LVDT, model LBB-375-TA-100, Lucas Schaevitz, Pennsauken, NJ). Engineering shear strain on the gage length surface γ was calculated based on the deflections of the LVDT's δ_1 and δ_2, the axial distance between the two rings L, the distances between the specimen surface and the point of contact of each LVDT with its aluminum tab t_1, t_2, and the radius of the specimen r using the following equation:

$$\gamma = \left[\arctan\left(\frac{\delta_1}{r + t_1}\right) - \arctan\left(\frac{\delta_2}{r + t_2}\right)\right]\frac{r}{L}. \quad (1)$$

Validation was accomplished by comparing elastic strains measured with this system to those measured using a rosette strain gage glued to a 6 mm diameter reduced-section aluminum specimen. Ten non-destructive torsional tests were performed with repositioning of the rotational transducer system between each test. The mean ($\pm$ S.D.) percent difference between the strain gage measurement of strain and the rotational transducer system measurement for the 10 tests (1.7% $\pm$ 1.0%, range from $-$ 3.4% to 2.0%) was not statistically different from zero ($p = 0.24$), confirming the system's accuracy with respect to the strain gage. The coefficient of variation of the rotational transducer system measurement on the aluminum specimen was 1.9%, demonstrating its repeatability. The shear modulus of one randomly chosen bovine tibial trabecular bone specimen was also measured six times with repositioning of the transducer system each time, yielding a coefficient of variation on trabecular bone of 4.5%. Based on these data, we considered our system to be accurate and precise for bovine trabecular bone.

Young's modulus was measured non-destructively in compression using a uniaxial servo-hydraulic load frame (Model 1331, Instron Corp., Canton, MA). Specimen diameter was measured six times with a digital caliper. Specimens were instrumented with a 5 mm gage length, 16 g extensometer (Model 632-29C-30, MTS, Minneapolis, MN) and loaded from 0% to 0.4% and back to 0% strain four times with the extensometer repositioned 90° circumferentially each time. Young's modulus was defined as the mean of the slopes of the resulting stress–strain curves between 0.1% and 0.4% strain (Keaveny *et al.*, 1994c).

After overnight storage at 2°C, specimens were tested to failure in torsion at room temperature using a biaxial servo-hydraulic load frame (Series 3300, Interlaken Corp., Minneapolis, MN). The rotational transducer system was mounted onto each specimen, and the axial distance between the two rings was determined using the mean of six measurements with a digital caliper. The end-caps were then gripped in the test frame with zero

axial load and torque. Angular displacement was applied at a rate of 2° per second [rate of approximately 0.6% strain per second, similar to the rate of 0.5% strain per second used in previous experiments (Keaveny *et al.*, 1994c)] up to an angular displacement of at least 30° to ensure reaching the ultimate torque. Torque was measured using a multicomponent force transducer (Model MC3A-6-500, Advanced Mechanical Technology, Inc., Newton, MA).

After mechanical testing, a low speed diamond saw (Labcut 1010, Extec, Enfield, CT) was used to section out a cylinder (approximately 5 mm in length) from one or both sides of the fracture site, depending on the amount of intact bone remaining in the gage length. The height and diameter of each cylinder were measured six times using a digital caliper. Marrow was removed from the cylinders using at least five 10-min cycles in an ultrasonic cleaner with a 1 : 3 bleach : water solution, with a water jet rinse after each cycle. The cylinders were centrifuged for 15 min at 1000 rpm and weighed to calculate wet apparent density.

Shear stress τ was determined from the torque vs angle of twist curve using the following equation (Nadai, 1950):

$$\tau = \frac{1}{2\pi r^3}\left[\theta\frac{dT}{d\theta} + 3T\right], \quad (2)$$

where T is the measured torque, r is the radius of the specimen, and θ is the angle of twist per unit length. The term $dT/d\theta$ was determined by fitting a fifth-degree polynomial to the torque vs angle of twist curve. Although the derivation of equation (2) assumes material isotropy, the errors associated with use of this equation should be minimal since our specimens were approximately transversely isotropic and trabeculae were aligned either parallel or perpendicular to the axis of the specimen. Shear strain at the specimen surface was calculated using equation (1). Shear modulus was defined as the slope of the stress–strain curve between 0.1% and 0.4% strain (Keaveny *et al.*, 1994c). The elastic range was the strain at which a line drawn from the origin with a slope equal to 95% of the shear modulus intersected the stress–strain curve. The yield stress and yield strain of each specimen were defined by the intersection of the stress–strain curve with a line parallel to the line defining shear modulus, but offset by 0.2% strain. The ultimate stress was the maximum stress; the ultimate strain was the lowest strain corresponding to the ultimate stress.

Six specimens were lost during testing, leaving 48 specimens (from 36 different tibiae; $n = 25$ longitudinal; $n = 23$ transverse) for statistical analysis. Reasons for lost specimens were: (1) insufficient gage length for proper rotational transducer placement (two transverse); (2) specimen mishandling (two longitudinal, one transverse); and (3) operator error (one longitudinal). Although four longitudinal and nine transverse specimens fractured outside the gage length, the stress–strain curves for these specimens indicated that the fractures occurred after the ultimate stress had been reached within the gage length. Thus, we obtained valid yield and ultimate data for all 48 specimens.

An unpaired Student's t-test indicated that the mean apparent density in the transverse group ($0.59 \pm 0.11\,g\,cm^{-3}$) was 18% higher ($p = 0.008$) than in the longitudinal group ($0.50 \pm 0.11\,g\,cm^{-3}$). Thus, comparisons between failure stresses were based on mean values adjusted for apparent density, using analyses of covariance with apparent density as covariate (RS1 version 4.3, BBN Software, Cambridge, MA). Unpaired t-tests were used to detect any dependence of failure strains on the trabecular orientation, since these properties did not depend on apparent density (see below). Linear regression analysis was used to determine relationships between shear failure properties, shear modulus and apparent density.

By combining our shear yield stresses with tensile and compressive yield stresses determined from previous experiments (Keaveny *et al.*, 1994c; unpublished data), we predicted yield stresses for off-axis compressive loads acting from 0° to 90° relative to the primary orientation using a maximum stress (Jones, 1975) and a Tsai–Wu failure criterion (Tsai and Wu, 1971). Under the maximum stress criterion, yielding was predicted when either: (1) the normal stress in the longitudinal direction exceeded the longitudinal yield stress, (2) the normal stress in the transverse direction exceeded the transverse yield stress, or (3) the shear stress exceeded the shear yield stress. Therefore, the predicted yield stress was the minimum of

$$\sigma = \frac{X_c}{\cos^2\theta}, \quad \sigma = \frac{Y_c}{\sin^2\theta} \quad \text{and} \quad \sigma = \frac{S}{\sin\theta\cos\theta}, \quad (3)$$

where σ is the applied off-axis compressive stress, θ is the angle between the applied stress and the primary trabecular orientation, X_c is the longitudinal compressive yield stress (22.65 MPa, Keaveny *et al.*, 1994c), Y_c is the transverse compressive yield stress (7.58 MPa, unpublished data), and S is the transverse shear yield stress (4.76 MPa). All yield stress values were based on a linear regression between yield stress and apparent density, evaluated at an overall mean apparent density of $0.62\,g\,cm^{-3}$. Although the maximum stress criterion does not allow for interactions between different failure modes, it provides insight into the dominant mode of failure for a given loading condition since it is simple to separate the contributions of each failure mode. To allow for interactions between failure modes and therefore provide a more realistic prediction of off-axis behavior, we also predicted off-axis yield stresses using the more complex Tsai–Wu criterion. For a transversely isotropic material under an off-axis compressive load, the Tsai–Wu failure criterion was reduced to

$$\left(\frac{1}{X_t} - \frac{1}{X_c}\right)\sigma\cos^2\theta + \left(\frac{1}{Y_t} - \frac{1}{Y_c}\right)\sigma\sin^2\theta + \frac{1}{X_tX_c}\sigma^2\cos^4\theta + \frac{1}{Y_tY_c}\sigma^2\sin^4\theta + \frac{1}{S^2}\sigma^2\sin^2\theta\cos^2\theta + 2F_{12}\sigma^2\sin^2\theta\cos^2\theta = 1, \quad (4)$$

where X_t is the longitudinal tensile yield strength (16.22 MPa, Keaveny *et al.*, 1994c), and Y_t is the transverse tensile yield strength (2.80 MPa, unpublished data). The value of F_{12}, the strength interaction term, was chosen as $-0.0108\,\text{MPa}^{-2}$ (Keaveny *et al.*, 1996). To investigate the relative contribution of shear to the off-axis failure properties, we predicted the off-axis yield stress using our measured shear yield stress value (adjusted to a mean density of $0.62\,\text{g cm}^{-3}$) of 4.76 MPa, and also using values 30% above (6.19 MPa) and 30% below (3.33 MPa) our measured value, while keeping all other properties constant.

RESULTS

All stress–strain curves were linear initially, followed by a gradual yield region until the ultimate point was reached (Fig. 3). Since the theory used to calculate the stress–strain curves is not valid beyond the ultimate point, we could not draw conclusions about stress–strain behavior beyond the ultimate point. However, we noted that specimens carried one-third to two-thirds of the ultimate torque when the limit of the rotational transducer system was reached (approximately 15% strain). Since all bone throughout the cross-section has yielded when the maximum torque is reached, this behavior suggests that there is a substantial load-carrying capacity after shear failure. Fracture lines were generally oblique (at approximately 45°) in the longitudinal group, and were either oblique or perpendicular to the specimen axis in the transverse group.

While shear failure stresses were heterogeneous (i.e. dependent on apparent density and shear modulus) as expected, shear failure strains were homogeneous (i.e. independent of apparent density and shear modulus). Shear yield and ultimate stresses were positively and linearly correlated with apparent density ($r^2 = 0.61 - 0.80$, Fig. 4, Table 1), and the slopes of the relationships were statistically similar ($p = 0.20$ and 0.36) for longitudinal vs transverse trabecular orientations. By contrast to the failure stresses, shear failure strains were independent of apparent density (Fig. 5, Table 1). Similar but stronger relationships were observed for failure stresses with shear modulus as the independent variable. There were weak negative correlations (longitudinal, $r^2 = 0.25$, $p = 0.01$; transverse, $r^2 = 0.20$, $p = 0.03$) between yield strain and shear modulus and between ultimate strain and shear modulus in the longitudinal group ($r^2 = 0.35$, $p = 0.002$, Table 1).

While yield and ultimate stresses were highly anisotropic, ultimate strains were isotropic and yield strains were only slightly anisotropic (Table 2). Mean ($\pm$ S.D.) values of shear yield and ultimate stress for the longitudinal orientation were 4.24 ± 1.42 MPa and 6.35 ± 2.00 MPa respectively; after adjusting for apparent density, these values were 62% and 61% higher respectively ($p < 0.0001$) than for the transverse orientation. The mean shear yield strain for the longitudinal orientation was $1.46 \pm 0.19\%$, which was 10% higher ($p = 0.01$) than for the transverse orientation ($1.33 \pm 0.15\%$). By contrast to the yield strains, there was no difference ($p = 0.24$) between the mean ultimate strains for longitudinal ($4.60 \pm 0.77\%$) vs transverse ($4.24 \pm 1.25\%$) trabecular orientations.

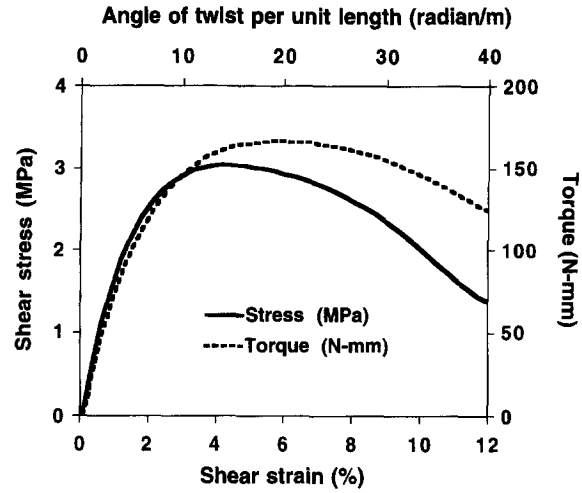

Fig. 3. Typical stress–strain and torque vs angle of twist (per unit length) curve for a longitudinal specimen. All specimens exhibited linear behavior initially, and yielded between 1.05% and 1.78% strain. The equation used to calculate stress from torque is not valid beyond the ultimate point. However, specimens typically carried one-third to two-thirds of the ultimate torque when the limit of the rotational transducer system was reached (approximately 15% strain), suggesting that there is a load-carrying capacity after the ultimate stress in shear.

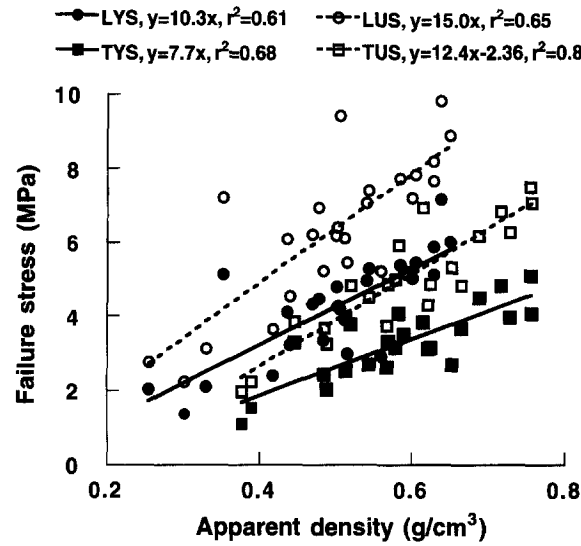

Fig. 4. Plots of yield and ultimate stress against apparent density for longitudinal and transverse trabecular orientations. LYS, longitudinal yield stress; TYS, transverse yield stress; LUS, longitudinal ultimate stress; TUS, transverse ultimate stress. For both yield and ultimate stress, the slopes of the relationships were statistically similar for the two trabecular orientations, although the adjusted mean ($\pm$ S.E.M.) yield and ultimate stresses for the longitudinal group (4.61 ± 0.16 MPa and 6.92 ± 0.21 MPa) were 62% and 61% higher, respectively ($p < 0.0001$, analysis of covariance with apparent density as covariate) than for the transverse group (2.85 ± 0.17 MPa and 4.30 ± 0.22 MPa).

Table 1. Linear regressions ($Y = aX + b$) of shear properties against apparent density (ρ, g cm^{-3}) and either shear modulus (G, GPa) or Young's modulus (E, MPa), compared for longitudinal and transverse trabecular orientations. Relationships for failure stresses (τ, MPa) had statistically similar slopes in the longitudinal and transverse groups (analysis of covariance, $p > 0.05$). Failure strains (γ, %) were independent of apparent density and only weakly dependent on shear modulus

		Longitudinal			Transverse		
Y	X	Slope	Intercept*	r^2	Slope	Intercept*	r^2
Shear modulus (MPa)	ρ	931	—	0.61	775	− 158	0.64
	E	0.143	—	0.78	0.351	—	0.67
Elastic range (%)	G	—	—	—	—	—	—
	ρ	—	—	—	—	—	—
τ_{yield} (MPa)	G	9.88	—	0.80	8.72	0.681	0.83
	ρ	10.3	—	0.61	7.67	—	0.68
γ_{yield} (%)	G	− 0.756	1.72	0.25	− 0.647	1.52	0.20
	ρ	—	—	—	—	—	—
$\tau_{ultimate}$ (MPa)	G	14.2	1.39	0.83	13.1	1.04	0.84
	ρ	15.0	—	0.65	12.4	− 2.36	0.80
$\gamma_{ultimate}$ (%)	G	− 3.52	5.82	0.35	—	—	—
	ρ	—	—	—	—	—	—

* Intercepts are only reported when significantly different from zero ($p < 0.05$).
— regression was not significant ($p > 0.05$).

Table 2. Comparison of mean values of the material properties for longitudinal and transverse trabecular orientations. All material properties, except apparent density and ultimate strain, were significantly lower for the transverse group

Material property	Longitudinal ($n = 25$) mean ± S.D. range adjusted mean (S.E.M.)*	Transverse ($n = 23$) mean ± S.D. range adjusted mean (S.E.M.)*	Transverse to longitudinal ratio†
Apparent density (g cm^{-3})	0.50 ± 0.11 0.25 − 0.65	0.59 ± 0.11 0.38 − 0.76	1.18‡
Shear modulus (MPa)	349 ± 128 99 − 535 384 (15)	296 ± 103 95 − 546 257 (16)	0.67¶
Young's modulus (MPa)	2470 ± 789 704 − 3700	719 ± 241 306 − 1300	0.29¶
Failure stresses (MPa):			
Yield stress	4.24 ± 1.42 1.37 − 7.18 4.61 (0.16)	3.26 ± 0.99 1.11 − 5.10 2.85 (0.17)	0.62¶
Ultimate stress	6.35 ± 2.00 2.22 − 9.83 6.92 (0.21)	4.92 ± 1.48 1.96 − 7.53 4.30 (0.22)	0.62¶
Failure strains (%)			
Elastic range	0.97 ± 0.23 0.46 − 1.35	0.80 ± 0.22 0.45 − 1.21	0.82‖
Yield strain	1.46 ± 0.19 1.07 − 1.78	1.33 ± 0.15 1.05 − 1.56	0.91‖
Ultimate strain	4.60 ± 0.77 2.96 − 6.00	4.24 ± 1.25 2.16 − 7.17	0.92 (No difference)**

* Adjusted means are only reported for properties where the slopes of the relationships with density were statistically similar for longitudinal and transverse loading (by analysis of covariance with density as covariate).
† Ratios are based on adjusted means for shear modulus and failure stresses; for Young's modulus and failure strains, comparisons were based on unpaired t-tests.
‡ $p = 0.008$;
¶ $p < 0.0001$;
‖ $p = 0.01$;
** $p = 0.2$.

The dominant failure mode for off-axis compressive loading depended on the angle between the applied load and the primary trabecular orientation (Fig. 6). Using the maximum stress criterion and the measured shear yield stress of 4.76 MPa, yielding in shear was predicted for angles between 11° and 56°, while yielding due to compressive stresses was predicted for all other angles [Fig. 6(B)]. When the shear yield stress was increased by 30%

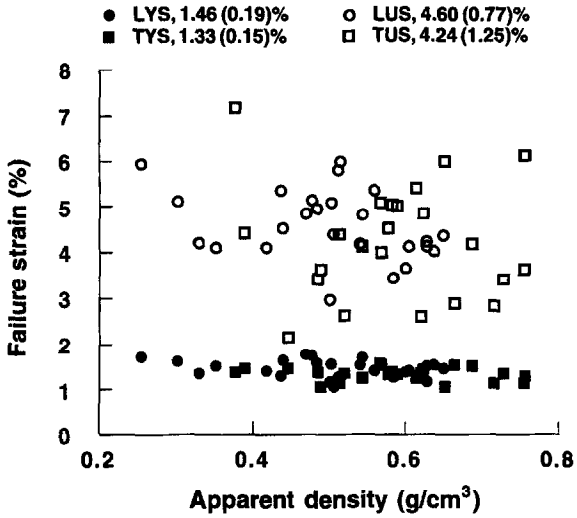

Fig. 5. Plots of yield and ultimate strain against apparent density for longitudinal and transverse trabecular orientations. LYS, longitudinal yield strain; TYS, transverse yield strain; LUS, longitudinal ultimate strain; TUS, transverse ultimate strain; numbers are mean (S.D.). Yield and ultimate strains were independent of apparent density in both groups. The mean ($\pm$ S.D.) yield strain for longitudinal loading ($1.46 \pm 0.19\%$) was 10% higher ($p = 0.01$, Student's t-test) than for transverse loading ($1.33 \pm 0.15\%$), indicating that shear yield strains were slightly anisotropic. However, there was no significant difference ($p = 0.20$) between the ultimate strains for the longitudinal ($4.60 \pm 0.77\%$) and transverse ($4.24 \pm 1.25\%$) trabecular orientations, indicating that the ultimate strains were isotropic.

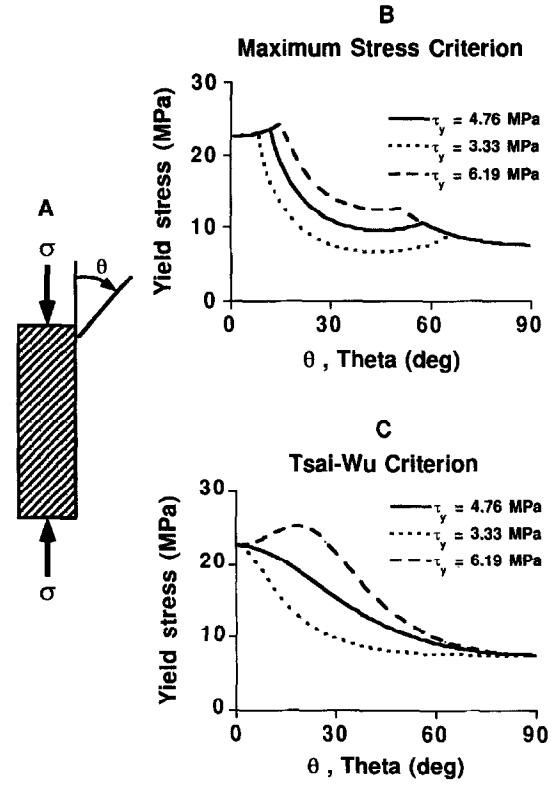

Fig. 6. (A) Yield stresses were predicted for uniaxial compressive stresses σ acting from $\theta = 0°$ (longitudinal loading) to $\theta = 90°$ (transverse loading) relative to the primary trabecular orientation, using our measured shear yield strength (4.76 MPa), and also using values 30% above (6.19 MPa) and 30% below (3.33 MPa) the mean value. Using the maximum stress criterion (B) and the measured shear yield stress of 4.76 MPa, yielding in shear was predicted for angles between 11° and 56°; when the shear yield stress was increased, yielding in shear was predicted for a smaller range of angles (15°–49°); when the shear yield stress was reduced, yielding in shear was predicted for a larger range of angles (8°–65°). The predicted yield stresses from the maximum stress criterion follow trends similar to those based on the more complex and realistic Tsai–Wu criterion (C), which also predicts large changes in off-axis yield stress with changes in the ratio of shear to compressive yield stress. These results indicate that shear is a dominant failure mode for a substantial range of off-axis loading directions, and that this range is dependent on the magnitude of the shear yield stress.

(therefore increasing the ratio of shear to compressive yield stress), yielding in shear was predicted for a slightly smaller range of angles (15°–49°); when the shear yield stress was reduced by 30%, yielding in shear was predicted for a larger range of angles (8°–65°). Although the maximum stress criterion did not allow for interaction between failure modes (as evidenced by slope discontinuities), the predicted yield stresses follow trends similar to those calculated from the more realistic Tsai–Wu criterion [Fig. 6(C)]. Thus, for compressive loads that are approximately 11°–56° oblique to the primary trabecular orientation, the dominant failure mode will be shear.

DISCUSSION

Based on trends we have measured for tensile and compressive failure of bovine tibial trabecular bone (Keaveny *et al.*, 1994b, c), we hypothesized in this study that shear failure strains of bovine tibial trabecular bone are homogeneous and isotropic. We also hypothesized that shear is a dominant failure mode when trabecular bone is loaded obliquely relative to its primary trabecular orientation. We found that while failure stresses in shear were highly inhomogeneous and anisotropic, shear failure strains were homogeneous and were either isotropic (ultimate) or only slightly anisotropic (yield). These results indicate that failure in shear can be predicted for (bovine tibial) trabecular bone of any density and orientation with knowledge of only its failure strains. We also predicted that shear failure dominates trabecular bone failure for a substantial range of off-axis compressive loading directions, and that this range depends on the magnitude of the shear yield stress.

Our use of a custom rotational displacement transducer system and a reduced-section cylindrical geometry enabled us to eliminate end-artifacts and bias failure to a region of constant surface stress, resulting in an unprecedented level of accuracy in the measurement of trabecular bone shear properties. By harvesting specimens from 36 different bones, our data also provide a good representation of the behavior of bovine proximal tibial bone in general. Since we were unable to randomly

Table 3. Comparison of our data for shear modulus and ultimate strength to those of previous investigators. In general, the agreement between studies is good despite differences in species and anatomic site

Study	Species, site and orientation (sample size)	Apparent density ($g\,cm^{-3}$) (mean ± S.D.)	Shear modulus (MPa) (mean ± S.D.)	Shear ultimate strength (MPa) (mean ± S.D.)
Stone *et al.* (1983)†	Bovine proximal humerus, along humeral axis ($n = 9$)	0.48*	—	6.60 ± 1.66
Saha and Gorman (1981)‡	Human proximal femur, embalmed, orientation not reported ($n = 11$)	0.44*	—	4.64 ± 3.10
	Human distal femur, embalmed, orientation not reported ($n = 25$)	0.40*	—	3.65 ± 1.90
Ashman *et al.* (1987)	Bovine proximal and distal femur, orientation not reported ($n = 13$)	0.54 ± 0.16	333 ± 152¶ 311 ± 114‖	—
Currrent study	Bovine proximal tibia, longitudinal ($n = 25$)	0.50 ± 0.11	349 ± 128	6.35 ± 1.89
	Bovine proximal tibia, transverse ($n = 23$)	0.59 ± 0.11	296 ± 103	4.92 ± 1.43

*Standard deviation not reported. — data not reported.
†Butterfly shaped specimens tested in a plane-stress testing device.
‡Rectangular specimens used; testing method was not reported.
¶Cylindrical specimens tested in torsion.
‖Shear modulus measured ultrasonically.

select longitudinal and transverse specimens from identical sites within the tibia, there may be architectural differences between groups which introduced a bias into our comparisons for different orientations. However, the most structurally important differences between groups were in apparent density and the direction of the primary trabecular orientation. Since we adjusted failure strengths for inter-group differences in apparent density, we believe that our comparisons for different trabecular orientations closely reflect the anisotropy of trabecular bone. It should also be noted that the absolute values of the reported properties may be somewhat inaccurate relative to the *in vivo* situation because *in vivo* boundary conditions can never be simulated exactly with excised trabecular bone specimens.

One possible limitation of our results is their applicability to human bone, due to differences in apparent density and architecture between human and bovine bone. The mean (± S.D.) wet apparent density of $0.54 \pm 0.11\,g\,cm^{-3}$ of our specimens is higher than those reported for the human lumbar spine, $0.19 \pm 0.08\,g\,cm^{-3}$* (Hansson *et al.*, 1987) and proximal tibia, $0.26 \pm 0.14\,g\,cm^{-3}$* (Ashman *et al.*, 1989), although our densities are similar to those reported for the human proximal femur, $0.50 \pm 0.16\,g\,cm^{-3}$* (Rohlmann *et al.*, 1980). Since failure stresses are highly dependent on apparent density, our failure stress results should be extrapolated carefully (if at all) to densities below our measured values. However, since we found that failure strains are independent of apparent density, our mean failure strain values may apply to low density human bone. Differences in architecture must also be considered when extrapolating our results to human bone, since the failure mechanisms at the trabecular level may differ. The substantial overlap of failure strains for longitudinal and transverse trabecular orientations, however, suggests that shear failure strains may be independent of architecture.

Our mean values for ultimate shear stress and shear modulus agree with values reported by previous investigators (Table 3). Our mean ultimate strength for longitudinal specimens (6.35 ± 1.89 MPa) agrees best with the value of 6.60 ± 1.66 MPa reported by Stone *et al.* (1983) for bovine humeral bone, most likely due to similarities in density and trabecular orientation between the two studies. The slightly lower values reported by Saha and Gorman (1981) are probably due to their use of lower density human bone. Our shear modulus values also compare favorably with those measured by ultrasound for the bovine femur (Ashman *et al.*, 1987). Although values for shear failure stains have not been reported, previous investigators have concluded that compressive failure strains are isotropic (Turner, 1989) or slightly anisotropic (Mosekilde *et al.*, 1987), which is in general consistent with our results for shear failure strains.

Our prediction that shear can dominate failure during off-axis loading may have implications for traumatic failure of bones, particularly age-related hip fractures. Although our analysis using the maximum stress criterion did not take into account interactions between failure modes [as evidenced by slope discontinuities in Fig. 6(B)], the predictions are consistent with those based on the more realistic Tsai–Wu criterion. Therefore,

*Dry apparent density values reported in these studies were converted to wet apparent density based on the data of Galante *et al.* (1970).

although one mode is not necessarily solely responsible for failure, our results indicate that shear can dominate trabecular bone failure for a relatively large range of off-axis loading directions. If this prediction holds for human bone, then failure of trabecular bone *in vivo* during traumatic, off-axis loading (such as in the proximal femur during falls) may be dominated by shear failure. Our results also indicate that if changes in trabecular structure with aging degrade shear properties more than compressive properties – which may occur as the body attempts to maintain maximum structural capacity for habitual activities – then shear will dominate trabecular bone failure for an even larger range of off-axis loading. Therefore, efforts to understand and predict the failure properties of the proximal femur under traumatic loading conditions may be improved by considering the shear as well as compressive properties of the trabecular bone.

Acknowledgements—This work was supported by the Whitaker Foundation, the Harvard–MIT Division of Health Sciences and Technology, the National Science Foundation, and the American Association of University Women.

REFERENCES

Ashman, R. B., Corin, J. D. and Turner, C. H. (1987) Elastic properties of cancellous bone: measurement by an ultrasonic technique. *J. Biomechanics* **20,** 979–986.

Ashman, R. B., Rho J. Y. and Turner, C. H. (1989) Anatomical variation of orthotropic elastic moduli of the proximal human tibia. *J. Biomechanics* **22,** 895–900.

Cheal, E. J., Spector, M. and Hayes, W. C. (1992) Role of loads and prosthesis material properties on the mechanics of the proximal femur after total hip arthroplasty. *J. Orthop. Res.* **10,** 405–422.

Halawa, M., Lee, A. J. C., Ling, R. S. M. and Vangala, S. S. (1978) The shear strength of trabecular bone from the femur, and some factors affecting the shear strength of the cement-bone interface. *Arch. Orthop. Traumat. Surg.* **92,** 19–30.

Hansson, T., Keller, T. and Panjabi, M. (1987) A study of the compressive properties of lumbar vertebral trabeculae: Effects of tissue characteristics. *Spine* **12,** 56–62.

Hvid, I., Bentzen, S. M., Linde, F., Mosekilde, L. and Pongsoipetch, B. (1989) X-ray quantitative computed tomography: the relations to physical properties of proximal tibial trabecular bone specimens. *J. Biomechanics* **22,** 837–844.

Hvid, I., Jensen, N., Bunger, C., Solund, K. and Djurhuus, J. (1985) Bone mineral assay: its relation to the mechanical strength of cancellous bone. *Engng Med.* **14,** 79–83.

Jones, R. (1975) Maximum stress theory. In *Mechanics of Composite Materials*, pp. 72–74. Scripta Book Company, Washington, D.C.

Keaveny, T., Wachtel, E. and Zadesky, S. (1996) Multiaxial failure characteristics of trabecular bone. *Trans. 42nd Orthop. Res. Soc.* **21,** 81.

Keaveny, T. M., Guo, X. E., Wachtel, E. F., McMahon, T. A. and Hayes, W. C. (1994a) Trabecular bone exhibits fully linear elastic behavior and yields at low strains. *J. Biomechanics* **27,** 1127–1136.

Keaveny, T. M., Wachtel, E. F., Cutler, M. J. and Pinilla, T. P. (1994b) Yield strains for bovine trabecular bone are isotropic but asymmetric. *Trans 40th Orthop. Res. Soc.* **19,** 428.

Keaveny, T. M., Wachtel, E. F., Ford, C. M. and Hayes, W. C. (1994c) Differences between the tensile and compressive strengths of bovine tibial trabecular bone depend on modulus. *J. Biomechanics* **27,** 1137–1146.

Lotz, J. C., Cheal, E. J. and Hayes, W. C. (1991) Fracture prediction for the proximal femur using finite element models: Part 1 – Linear analysis. *J. Biomech. Engng* **113,** 353–360.

Mosekilde, L., Mosekilde, L. and Danielsen, C. (1987) Biomechanical competence of vertebral trabecular bone in relation to ash density and age in normal individuals. *Bone* **8,** 79–85.

Nadai, A. (1950) Torsion of a round bar. The stress–strain curve in shear. In *Theory of Flow and Fracture of Solids*. McGraw-Hill, New York.

Rohl, L., Larsen, E., Linde, F., Odgaard, A. and Jorgensen, J. (1991) Tensile and compressive properties of cancellous bone. *J. Biomechanics* **24,** 1143–1149.

Rohlmann, A., Zilch, H., Bergmann, G. and Kolbel, R. (1980) Material properties of femoral cancellous bone in axial loading. Part I: Time independent properties. *Arch. Orthop. Traumat. Surg.* **97,** 95–102.

Saha, S. and Gorman, P. H. (1981) Strength of human cancellous bone in shear and its relationship to bone mineral content. *Trans. 27th Orthop. Res. Soc.* **6,** 217.

Stone, J. L., Beaupre, G. S. and Hayes, W. C. (1983) Multiaxial strength characteristics of trabecular bone. *J. Biomechanics* **16,** 743–752.

Tsai, S. W. and Wu, E. M. (1971) A general theory of strength for anisotropic materials. *J. Comp. Mater.* **5,** 58–80.

Turner, C. (1989) Yield behavior of bovine cancellous bone. *J. Biomech. Engng* **111,** 256–260.